Quintessence and gravitational waves

Alain Riazuelo*
Département d'Astrophysique Relativiste et de Cosmologie, CNRS-UMR 8629, Observatoire de Paris, F-92195 Meudon, France

Jean-Philippe Uzan†
Laboratoire de Physique Théorique, CNRS-UMR 8627, Université Paris XI, Bât. 210, F-91405 Orsay Cedex, France
and Département de Physique Théorique, Université de Genève, 24 quai E. Ansermet, CH-1211 Genève 4, Switzerland
(Received 12 April 2000; published 25 September 2000)

We investigate some aspects of quintessence models with a nonminimally coupled scalar field and in particular we show that it can behave as a component of matter with $-3\leq P/\rho\leq 0$. We study the properties of gravitational waves in this class of models and discuss their energy spectrum and the cosmic microwave background anisotropies they induce. We also show that gravitational waves are damped by the anisotropic stress of the radiation and that their energy spectrum may help to distinguish between the inverse power law potential and supergravity motivated potential. We finish with a discussion on the constraints arising from their density parameter $\Omega_{\rm GW}$.

PACS number(s): 98.80.Cq

I. INTRODUCTION

Recent astrophysical and cosmological observations such as the luminosity distance-redshift relation for supernovae type Ia [1–3], the recent observations of the cosmic microwave background temperature anisotropies [4], gravitional lensing [5], and velocity fields [6] tend to indicate that a large fraction of the matter of the universe today is composed of matter with negative pressure (see, e.g., Ref. [7] for a comparison of the different observations). Recent analyses [8,9] seem to indicate that the energy density ρ and the pressure P of this fluid satisfies

$$-1\leq P/\rho\leq -0.6, \tag{1}$$

which is compatible with a cosmological constant Λ for which $P/\rho=-1$ (see also Ref. [10] for arguments in favor of $P/\rho<-1$). A typical value of $\Omega_\Lambda\simeq 0.7$ for its energy density in units of the critical density of the universe corresponds to an energy scale of order 5×10^{-47} GeV^4 which is very far from what is expected from high energy physics; this is the well known cosmological constant problem [11]. To circumvent this problem different solutions have been proposed starting from the idea of a dynamical cosmological constant [12] and leading to the class of models known as *quintessence* [13], where a spatially homogeneous scalar field ϕ is rolling down a potential decreasing when ϕ tends to infinity. An example of such a potential which has been widely studied is the inverse power law potential. It can be obtained from some high-energy physics models, e.g., where supersymmetry is broken through fermion condensates [14]. Recently, it has been argued [15] that supergravity has to be taken into account since today one expects the scalar field to be of order of the Planck mass $M_{\rm pl}$ and corrections to the potential appear at this energy. This leads to a better agreement with observations [16].

An important point about this family of models is the existence of scaling solutions [17,18] (referred to as *tracking solutions*), i.e., such that ϕ evolves as the scale factor of the universe at a given power. These solutions are attractors of the dynamical system describing the evolution of the scale factor and of the scalar field. This implies that the present time behavior of the field is almost independent of its initial conditions [19,20]. This property allows us to address [21] (i) the coincidence problem, i.e., the fact that ϕ starts to dominate today and (ii) the fine tuning problem, i.e., the fact that one does not have to fine tune the initial condition of the field ϕ.

One of us extended these models to include a nonminimal coupling $\xi\bar{R}f(\phi)$ between the scalar field and the scalar curvature $\bar{R}$ [22]. Such a coupling term appears, e.g., when quantising fields in curved spacetime [23,24] and in multidimensional theories [25–27]. It was shown that when $f(\phi)=\phi^2/2$ tracking solutions still exist [22] and this result was generalized [28] to any coupling function f and potential V satisfying $V(\phi)\propto f^n(\phi)$. However, such a coupling is constrained by the variations of the constants of nature [29] which fix bounds on ξ [30]. A way to circumvent this problem is to consider quintessence models in the framework of scalar-tensor theories [31,32] where a double attractor mechanism can occur, i.e., of the scalar-tensor theory towards general relativity and of the scalar field ϕ towards its tracking solution.

Among all the possible observations of cosmology, gravitational waves give an insight on epochs where there was a variation of the background dynamics since every such variation affects the shape of the stochastic graviton background spectrum [33,34]. We can then view our universe as containing a sea of stochastic gravitational waves from primordial origin, as predicted by most models of structure formations such as inflation [33,34] (see also Ref. [35] for a

*Email address: Alain.Riazuelo@obspm.fr
†Email address: Jean-Philippe.Uzan@th.u-psud.fr

review) and topological defects scenarios [36]. Their spectrum extends typically from 10^{-18} Hz (for wavelengths of order of the size of the Hubble radius today) to $\simeq 10^{10}$ Hz (the smallest mode that has been inflated out of the Hubble radius) and they could be detected or constrained by coming experiments such as the Laser Interferometric Gravitational Wave Observatory (LIGO) [37], VIRGO [38] (at $\simeq 10^{2}$ Hz), and the Laser Interferometer Space Antenna (LISA) [39] (at $\simeq 10^{-4}$ Hz). Gravitational waves, which are perturbations in the metric of the universe have also an effect on the cosmic microwave (CMB) temperature anisotropy [40–44] and polarization [45] allowing to extract information on their amplitude from the measure of the CMB anisotropies. For instance, bounds on the energy density spectrum of these cosmological gravitational waves in units of the critical density, $\Omega_{\rm GW}$, have been obtained from the CMB [40–42]

$$\left.\frac{d\Omega_{\rm GW}}{d\ln\omega}\right|_{10^{-18}\,\rm Hz} \lesssim 10^{-10}.$$

Gravitational waves are also a very good probe of the conditions in the early universe since they decouple early in its history and can help, e.g., testing the initial conditions of ϕ. An example was put forward by Giovannini [46,47] who showed that in a class of quintessential inflation models [48] there was an era dominated by the scalar field ϕ before the radiation dominated era which implies that a large part of the gravitational wave energy of order $\Omega_{\rm GW}\simeq 10^{-6}$ (about eight orders of magnitude higher than for standard inflation) was in the GHz region. This may happen in any scenario where the inflation ends with a kinetic phase [24,49] or when the dominant energy condition is violated [50]. On the other hand, the CMB temperature fluctuations give information on the history of the gravitational waves in between the last scattering surface and today through the integrated Sachs-Wolfe effect, whereas the polarization of the CMB radiation gives mainly information on the gravitational waves at decoupling. These three observables (energy spectrum, CMB temperature and polarization anisotropies) are thus complementary and we aim to present here a global study of the cosmological properties of the gravitational waves.

The goals of this article are (i) to study in more details the cosmology with a nonminimal quintessence field and (ii) to study gravitational waves in this class of models. In Sec. II we set up the general framework and describe the two potentials we shall consider. In Sec. III we introduce and define the observable quantities associated with the gravitational waves: their energy density spectrum and their imprint on the CMB radiation anisotropies and its polarization. In Sec. IV, we point out the general mechanism of damping by the anisotropic stress of the radiation. In Sec. V we discuss the parameters of the problem and investigate the tuning of the potential parameters; we also describe the evolution of the background spacetime and show that a nonminimally coupled quintessence field is a candidate for a $(\omega<-1)$-matter. In Sec. VII we describe the main properties of the gravitational waves. We finish in Sec. VIII by presenting numerical results and we underline the complementarity of the different observational quantities.

This work gives a detailed study of the observational effects of gravitational waves in the framework of quintessence, including some recent developments, and allowing for nonminimal coupling. This extends the work on quintessential inflation [46] by including the effects on the CMB. It also extends the studies on the cold dark matter model with a cosmological constant (ΛCDM) [51] to quintessence and is, as far as we know, a more complete study of the effect of gravitational waves on the CMB polarization. We hope to show that a joint study of the gravitational wave detection experiments [37–39] of the CMB experiments [4,52,53] and of the polarization experiments [53] can lead to a better determination of their properties.

II. GENERAL FRAMEWORK

A. Background spacetime

We consider a universe described by a Friedmann-Lemaître model with Euclidean spatial sections so that the metric takes the form

$$ds^2=a^2(\eta)[-d\eta^2+\delta_{ij}dx^i dx^j]\equiv\overline{g}_{\mu\nu}dx^\mu dx^\nu, \qquad (2)$$

where a is the scale factor and η the conformal time. Greek indices run from 0 to 3 and latin indices from 1 to 3.

We assume that the matter content of the universe can be described by a mixure of matter and radiation (mainly baryons, CDM, photons and three families of massless, nondegenerate neutrinos) and a scalar field ϕ nonminimally coupled to gravity evolving in a potential $V(\phi)$ that will be described later. The action for this system is

$$S=\int d^4x\sqrt{-\overline{g}}\left[\frac{\overline{R}}{2\kappa}-\xi\overline{R}f(\phi)-\frac{1}{2}\partial_\mu\phi\partial^\mu\phi-V(\phi)+\mathcal{L}_{\rm matter}\right], \qquad (3)$$

with $\kappa\equiv 8\pi G$, G being the Newton constant, and where $\mathcal{L}_{\rm matter}$ is the Lagrangian of the ordinary matter which is uncoupled to the scalar field and $f(\phi)$ is an arbitrary function of the scalar field that will be specified later. The action (3) can be rewritten under the interesting form

$$S=\int d^4x\sqrt{-\overline{g}}\left[\frac{\overline{R}}{2\kappa_{\rm eff}[\phi]}-\frac{1}{2}\partial_\mu\phi\partial^\mu\phi-V(\phi)+\mathcal{L}_{\rm matter}\right], \qquad (4)$$

with

$$\kappa_{\rm eff}[\phi]\equiv\frac{\kappa}{1-2\xi\kappa f(\phi)}. \qquad (5)$$

The stress-energy tensor of the scalar field is obtained by varying its Lagrangian $[-\xi\overline{R}f(\phi)-\frac{1}{2}\partial_\mu\phi\partial^\mu\phi-V(\phi)]$ to get

$$T^{(\phi)}_{\mu\nu}=\bar{\nabla}_\mu\phi\bar{\nabla}_\nu\phi-\frac{1}{2}\bar{g}_{\mu\nu}\bar{\nabla}_\lambda\phi\bar{\nabla}^\lambda\phi-V(\phi)\bar{g}_{\mu\nu}$$
$$+2\xi[\bar{g}_{\mu\nu}\bar{\nabla}_\lambda\phi\bar{\nabla}^\lambda\phi-\bar{\nabla}_\mu\phi\bar{\nabla}_\nu\phi$$
$$-\phi\bar{\nabla}_\mu\bar{\nabla}_\nu\phi+\phi\bar{\Box}\phi\bar{g}_{\mu\nu}+\bar{G}_{\mu\nu}f(\phi)] \quad (6)$$

where $\bar{G}_{\mu\nu}$ is the Einstein tensor of the metric $\bar{g}_{\mu\nu}$, $\bar{\nabla}$ its covariant derivative and $\bar{\Box}\equiv\bar{\nabla}_\mu\bar{\nabla}^\mu$.

The equations governing the evolution of the background spacetime are then obtained by varying Eq. (3) with respect to $\bar{g}_{\mu\nu}$, ϕ and the ordinary matter fields to get, respectively, the Friedmann equations, the Klein-Gordon equation, and the fluid conservation equation

$$\mathcal{H}^2=\frac{\kappa a^2}{3}(\rho+\rho_\phi), \quad (7)$$

$$\dot{\mathcal{H}}-\mathcal{H}^2=-\frac{\kappa a^2}{2}(\rho+P+\rho_\phi+P_\phi), \quad (8)$$

$$\ddot{\phi}+2\mathcal{H}\dot{\phi}+a^2\frac{dV}{d\phi}+6\xi(2\mathcal{H}^2+\dot{\mathcal{H}})=0, \quad (9)$$

$$\dot{\rho}=-3\mathcal{H}(\rho+P). \quad (10)$$

An overdot denotes a derivative with respect to the conformal time and $\mathcal{H}\equiv\dot{a}/a$ is the comoving Hubble parameter. The matter fluid energy density ρ and pressure P are assumed to satisfy the equation of state $P=\omega\rho$. The factor ω varies from 1/3 deep in the radiation era to 0 in the matter era. The scalar field energy density ρ_ϕ and pressure P_ϕ are obtained from its stress-energy tensor (6) and are then explicitely given by

$$\rho_\phi=\frac{1}{2}\frac{\dot{\phi}^2}{a^2}+V(\phi)+\frac{2\xi}{a^2}[3\mathcal{H}^2f(\phi)+3\mathcal{H}\dot{f}(\phi)], \quad (11)$$

$$P_\phi=\frac{1}{2}\frac{\dot{\phi}^2}{a^2}-V(\phi)-\frac{2\xi}{a^2}[(2\dot{\mathcal{H}}+3\mathcal{H}^2)f(\phi)$$
$$+\mathcal{H}\dot{f}(\phi)+\ddot{f}(\phi)]. \quad (12)$$

We stress that the conservation equation derived from (6) reduces to the Klein-Gordon equation (9). For each matter component, X say, we introduce the density parameter Ω_X defined as

$$\Omega_X\equiv\frac{\kappa a^2\rho_X}{3\mathcal{H}^2}. \quad (13)$$

To completely specify the model, we have to fix the potential $V(\phi)$. Following our previous work [22] and as discussed in the introduction we choose it to behave as

$$V(\phi)=\Lambda^4\left(\frac{\Lambda}{\phi}\right)^\alpha, \quad \alpha>0, \quad (14)$$

where Λ is an energy scale. As shown in Ref. [22], such a potential leads to the existence of tracking solutions whatever the value of ξ and for which the scalar field behaves as a barotropic fluid of equation of state (as long as the background fluid dominates)

$$P_\phi=\omega_\phi\rho_\phi \text{ with } \omega_\phi=-1+\frac{\alpha(1+\omega)}{\alpha+2}. \quad (15)$$

We also consider another class of potentials arising when one takes supergravity into account [15,16] and given by

$$\tilde{V}(\phi)=\Lambda^4\left(\frac{\Lambda}{\phi}\right)^\alpha\exp(\kappa\phi^2/2), \quad \alpha>0. \quad (16)$$

The effect of the exponential term is important only at late time so that the scaling properties of the tracking solution are not affected during the matter and radiation era. However when the field starts to dominate it leads to its stabilization [16] which has an effect on the effective equation of state of the scalar fluid.

B. Gravitational waves

In this article, we want to focus on the properties of the gravitational waves which are tensorial perturbations. At linear order, the metric is expanded as

$$g_{\mu\nu}=\bar{g}_{\mu\nu}+f_{\mu\nu} \quad (17)$$

where $f_{\mu\nu}$ is a transverse traceless (TT) perturbation, i.e., satisfying

$$f_{00}=f_{0i}=0, \quad f_{\mu\nu}\bar{g}^{\mu\nu}=0, \quad \bar{\nabla}_\mu f^{\mu\nu}=0. \quad (18)$$

It is also useful to define the perturbation $h_{\mu\nu}$ by

$$f_{\mu\nu}\equiv a^2h_{\mu\nu} \quad (19)$$

which, from Eq. (18), satisfies

$$h_{00}=h_{0i}=0, \quad h_{kl}\delta^{kl}=0, \quad \partial_k h^{kl}=0. \quad (20)$$

The equation of evolution of h_{kl} is obtained by considering the TT part of the perturbed Einstein equation (see, e.g., Ref. [54]) which leads to

$$\ddot{h}_{kl}+2[\mathcal{H}-\kappa_{\rm eff}\xi\dot{f}(\phi)]\dot{h}_{kl}-\Delta h_{kl}=2\kappa Pa^2\bar{\pi}_{kl}, \quad (21)$$

where $\Delta\equiv\partial_i\partial^i$ is the Laplacian and where the anisotropic stress tensor of the matter $\bar{\pi}_{kl}$ is defined as the tensor component of the matter stress-energy tensor

$$\delta T^i_j\equiv P\bar{\pi}^i_j, \quad \bar{\pi}^k_k=\partial_i\bar{\pi}^i_k=0. \quad (22)$$

The anisotropic stress of the matter fluid is dominated by the contribution of the neutrinos and of the photons and its form can be obtained by describing these relativistic fluids by a Boltzmann equation [55] (see Sec. III B below).

III. OBSERVATIONAL QUANTITIES

The goal of this section is to define the observable quantities related to the gravitational waves. We start by reviewing the computation of the energy density $\rho_{\rm GW}$ of a stochastic background of gravitational waves and finish by describing their effect on the CMB radiation, namely, we present the computation of the coefficients C_l of the development of the angular correlation function of the CMB temperature anisotropy and polarization.

A. Gravitational waves energy density

The definition of the gravitational waves stress-energy tensor $t_{\mu\nu}$ can be found in, e.g., Ref. [11] in the case of a Minkowski background spacetime, in, e.g., Ref. [56] in the case of a Friedmann-Lemaître spacetime, and a general discussion can be found in, e.g., Ref. [57].

To define the gravitational waves stress-energy tensor, we have to expand the Einstein-Hilbert action (4) to second order in the perturbation $f_{\mu\nu}$, which implies to develop the curvature scalar R at second order in the perturbations (see Refs. [11,56,57]) to get (up to divergence terms and forgetting the contribution arising from $\mathcal{L}_{\rm matter}$)

$$\delta^{(2)}S=-\int\frac{1}{4\kappa_{\rm eff}[\phi]}\bar{\nabla}_\mu f_{\alpha\beta}\bar{\nabla}^\mu f^{\alpha\beta}\sqrt{-\bar{g}}d^4x. \tag{23}$$

This expression is valid whatever the background metric as long as $f_{\mu\nu}$ is a transverse traceless perturbation. Note that contrarily to the ''standard'' situation, κ now depends on ϕ because of the nonminimal coupling with the scalar field. Using the fact that $\nabla_\mu f_{\alpha\beta}=a^2\partial_\mu h_{\alpha\beta}$ we can rewrite the previous expression as

$$\delta^{(2)}S=-\int\frac{1}{4\kappa_{\rm eff}[\phi]}\partial_\mu h_{kl}\partial^\mu h^{kl}\sqrt{-\bar{g}}d^4x, \tag{24}$$

which assumes a Friedmann-Lemaître background and the decomposition (20). Now, we decompose h_{kl} on its two polarizations as

$$h_{kl}=\sum_{\lambda=+,\times}h^{(\lambda)}(\eta,\mathbf{x})\epsilon_{kl}^{(\lambda)}(\mathbf{x}), \tag{25}$$

where $\epsilon_{kl}^{(\lambda)}(\mathbf{x})$ is the polarization tensor defined as

$$\epsilon_{kl}^{(\lambda)}(\mathbf{x})\equiv(e_k^1e_l^1-e_k^2e_l^2)\delta_\times^\lambda+(e_k^1e_l^2+e_l^1e_k^2)\delta_+^\lambda \tag{26}$$

for a wave propagating along the direction $\mathbf{e}_3$ and where $(\mathbf{e}_1,\mathbf{e}_2,\mathbf{e}_3)$ is a local orthonormal basis. Since this basis and the polarization tensor satisfy

$$e_i^a e_b^i=\delta_b^a,\quad \epsilon_{kl}^{(\lambda)}\epsilon_{(\lambda')}^{kl}=2\delta_{\lambda'}^\lambda, \tag{27}$$

we can rewrite the action (24) of the graviton as

$$\delta^{(2)}S=-\sum_\lambda\int\frac{1}{2\kappa_{\rm eff}[\phi]}\partial_\mu h^{(\lambda)}\partial^\mu h^{(\lambda)}\sqrt{-\bar{g}}d^4x, \tag{28}$$

which is the action for two massless scalar fields h_λ evolving in the background spacetime, as first noticed by Grishchuk [33,34]. By varying this action with respect to the background metric, we then deduce the stress-energy tensor of the gravitational waves

$$t_{\mu\nu}=-\frac{1}{2\kappa_{\rm eff}[\phi]}\sum_\lambda(\partial_\mu h^{(\lambda)}\partial_\nu h^{(\lambda)}-\bar{g}_{\mu\nu}\partial_\alpha h^{(\lambda)}\partial^\alpha h^{(\lambda)}). \tag{29}$$

If we decompose $h^{(\lambda)}$ in Fourier modes as

$$h^{(\lambda)}(\mathbf{x},\eta)=\int\frac{d^3\mathbf{k}}{(2\pi)^3}\hat{h}^{(\lambda)}(\mathbf{k},\eta)e^{i\mathbf{k}.\mathbf{x}}, \tag{30}$$

we can relate $\hat{h}^{(\lambda)}(\mathbf{k},\eta)$ to its initial value $\hat{h}^{(\lambda)}(\mathbf{k},\eta_{\rm in})$, i.e., its value deep in the radiation era (e.g., at the end of the inflationary phase) through the transfer function $T(k,\eta)$ by solving Eq. (21) to get

$$\hat{h}^{(\lambda)}(\mathbf{k},\eta)=T(k,\eta)\hat{h}^{(\lambda)}(\mathbf{k},\eta_{\rm in}). \tag{31}$$

Defining the initial power spectrum of the tensor modes as

$$\langle\hat{h}^{(\lambda)}(\mathbf{k},\eta_{\rm in})\hat{h}^*_{(\lambda')}(\mathbf{k}',\eta_{\rm in})\rangle\equiv k^{-3}P_h(k)\delta(\mathbf{k}-\mathbf{k}')\delta^\lambda_{\lambda'}, \tag{32}$$

(δ is the Dirac distribution), we can express the space average of $t_0^0(\mathbf{x},\eta)$ as

$$\begin{aligned}-\langle t_0^0(\mathbf{x},\eta)\rangle&=\frac{1}{2\kappa_{\rm eff}[\phi]a^2}\sum_\lambda\langle\partial_i h^{(\lambda)}\partial_j h^{(\lambda)}\delta^{ij}\rangle\\&=\frac{1}{\kappa_{\rm eff}[\phi]}\int\frac{k^2}{2\pi a^2}P_h(k)T^2(k,\eta)d\ln(k),\end{aligned} \tag{33}$$

where we used an ergodic hypothesis to replace the space average by an ensemble average. Now, since $\langle t_0^0(\mathbf{x},\eta)\rangle$ oscillates, we define the energy density of the gravitational waves by taking the average of Eq. (33) over n periods. It follows that

$$\rho_{\rm GW}(\eta)=\frac{1}{\kappa_{\rm eff}[\phi]}\int\frac{k^2}{2\pi a^2}P_h(k)\overline{T^2}(k,\eta)d\ln(k), \tag{34}$$

where $\overline{T}(k,\eta)$ is the root mean square of $T(k,\eta)$ over n periods which is well defined as long as the amplitude of the wave varies slowly with respect to its period.

The energy density $\rho_{\rm GW}$ and energy density parameter $\Omega_{\rm GW}$ by frequency band are then obtained (after averaging on several periods of the wave) by

$$\frac{d\rho_{\rm GW}(k,\eta)}{d\ln(k)}=\frac{1}{2\pi^2\kappa_{\rm eff}[\phi]}\left(\frac{k}{a}\right)^2P_h(k)\overline{T^2}(k,\eta), \tag{35}$$

$$\frac{d\Omega_{\rm GW}(k,\eta)}{d\ln(k)}=\frac{1}{6\pi^2}\left(\frac{\kappa}{\kappa_{\rm eff}[\phi]}\right)\left(\frac{k}{\mathcal{H}}\right)^2 P_h(k)\overline{T^2}(k,\eta). \tag{36}$$

Let us stress some important points. Since we have to average on several periods, these expressions are valid only in a ''shortwave limit'' (see Ref. [57] for discussion) where (i) the amplitude of the perturbation is small and (ii) the wavelength of the wave is small compared to the typical radius of the background spacetime. In our case this can be rephrased as $k/\mathcal{H}>1$ which implies that the expressions (35) and (36) are valid only for modes which are ''subhorizon'' today, i.e., whose wavelength is smaller than the Hubble radius today. For such modes the ergodic hypothesis is well justified. In fact, because of the averaging procedure of the transfer function, we have to restrict to modes such that $k/\mathcal{H}_0 \gtrsim 60$ if we want to average on about ten periods. Again, we emphasize that there is an explicit dependence of $\Omega_{\rm GW}$ and $\rho_{\rm GW}$ on the scalar field ϕ because of the non-minimal coupling and our expressions reduce to the standard ones [11,35,43,44,46,57] when $\xi=0$. We have described the gravitational waves by two stochastic variables $\hat{h}^{(\lambda)}$ which can be understood as being the classical limit of a complete quantum description of the gravitational waves (see, e.g., Refs. [33,34,56] for details).

Before turning to the effects of the gravitational waves on the CMB, let us make a comment that will lead us to introduce some new notations. In the previous analysis we decomposed the metric perturbation h_{ij} on the basis $\tilde{Q}^{\lambda}_{ij}(\mathbf{x},\mathbf{k}) \equiv \epsilon^{\lambda}_{ij}\exp(i\mathbf{k}\cdot\mathbf{x})$ of TT eigenfunctions of the Laplacian, i.e., such that

$$\Delta\tilde{Q}^{\lambda}_{ij}=-k^2\tilde{Q}^{\lambda}_{ij} \quad \text{with} \quad \partial^i\tilde{Q}^{\lambda}_{ij}=\delta^{ij}\tilde{Q}^{\lambda}_{ij}=0. \tag{37}$$

Such a decomposition is indeed not unique and we could have chosen any other such basis. In the CMB literature, one often prefers [58] to use the basis $Q^{(\pm 2)}_{ij}(\mathbf{x},\mathbf{k})$ defined by

$$Q^{(\pm 2)}_{ij}\equiv-\sqrt{\frac{3}{8}}(e_1\pm ie_2)_i(e_1\pm ie_2)_j e^{i\mathbf{k}\cdot\mathbf{x}}, \tag{38}$$

the vectors e_1 and e_2 being defined above in Eq. (26). If we decompose h_{ij} on the latter basis as

$$h_{ij}=\sum_{m=\pm 2}\int\frac{d^3\mathbf{k}}{(2\pi)^3}2H^{(m)}Q^{(m)}_{ij}(\mathbf{x},\mathbf{k}), \tag{39}$$

then the two decompositions are related by

$$\hat{h}^{(\times)}=-\sqrt{\frac{3}{2}}[H^{(+2)}+H^{(-2)}],$$

$$\hat{h}^{(+)}=-\sqrt{\frac{3}{2}}i[H^{(+2)}-H^{(-2)}]. \tag{40}$$

The two polarizations $H^{(\pm 2)}$ are then solution of Eq. (21) which reads

$$\ddot{H}^{(m)}+2[\mathcal{H}-\kappa_{\rm eff}\xi\dot{f}(\phi)]\dot{H}^{(m)}+k^2H^{(m)}=\kappa P a^2\pi^{(m)}, \tag{41}$$

where $\pi^{(m)}$ is the coefficient of the development of δT_{ij} as in Eq. (39) so that the transfer functions for $H^{(m)}$ and $\hat{h}^{(\lambda)}$ are the same. If we now define the power spectrum of $H^{(m)}(\mathbf{k},\eta_{\rm in})$ as

$$\langle H^{(m_1)}(\mathbf{k},\eta_{\rm in})H^{(m_2)*}(\mathbf{k}',\eta_{\rm in})\rangle = (2\pi)^3k^{-3}P_T(k)\,\delta(\mathbf{k}-\mathbf{k}')\,\delta_{m_1,m_2} \tag{42}$$

one can easily check that

$$P_T(k)=\frac{1}{3}P_h(k) \tag{43}$$

and that if the two polarizations $+$ and $\times$ are independent then $H^{(+2)}$ and $H^{(-2)}$ are also independent. With these notations, the energy density spectra are given as

$$\frac{d\rho_{\rm GW}}{d\ln(k)}=\frac{3}{2\pi^2\kappa}\left(\frac{k}{a}\right)^2 P_T(k)\overline{T^2}(k,\eta), \tag{44}$$

$$\frac{d\Omega_{\rm GW}}{d\ln(k)}=\frac{1}{2\pi^2}\left(\frac{\kappa}{\kappa_{\rm eff}}\right)\left(\frac{k}{\mathcal{H}}\right)^2 P_T(k)\overline{T^2}(k,\eta). \tag{45}$$

Indeed, this does not change the result but we found interesting to make the link between the notations used in the gravitational waves literature [11,35,43,44,46,57] and in the CMB literature [45,58], specially because we want to present both in a unified framework and language. From now on, we use the second decomposition and its interest will be enlightened by the study of the CMB anisotropies.

B. CMB temperature and polarization anisotropies

Gravitational waves, being metric perturbations, have an effect on the temperature and polarization of the CMB photons. Any metric perturbation induces a fluctuation on the CMB temperature Θ through the Sachs-Wolfe effect [59] and any anisotropic distribution of photons scattered by electrons will become polarized and vice versa. Since Thomson scattering generates linear polarization, we only need to consider the Stokes parameters Q and U and more conveniently their two combinations $Q\pm iU$ which are invariant under rotation.

Following Hu and White [58], we decompose the tensorial part of the temperature anisotropies according to

$$\Theta(\eta,\mathbf{x},\hat{n}) = \int \frac{d^3\mathbf{k}}{(2\pi)^3} \sum_l \sum_{m=\pm 2} \Theta_l^{(m)}(k,\eta) G_l^m(\mathbf{k},\mathbf{x},\hat{n}), \tag{46}$$

$$(Q \pm iU)(\eta,\mathbf{x},\hat{n}) = \int \frac{d^3\mathbf{k}}{(2\pi)^3} \sum_l \sum_{m=\pm 2} (E_l^{(m)} \pm iB_l^{(m)})(k,\eta) \times {}_{\pm 2}G_l^m(\mathbf{k},\mathbf{x},\hat{n}). \tag{47}$$

The coefficients $E_l^{(m)}$ and $B_l^{(m)}$ transform as $E_l \to (-)^l E_l$ and $B_l \to -(-)^l B_l$ under parity and are called the ''electric'' and ''magnetic'' part of the polarization. The functions G_l^m, ${}_{\pm 2}G_l^m$ form three independent sets of orthonormal functions and depend both on the position $\mathbf{x}$ and on the direction of propagation of the photons $\hat{n}$ and are defined as

$$G_l^m(\mathbf{k},\mathbf{x},\hat{n}) \equiv (-)^l \sqrt{\frac{4\pi}{2l+1}} Y_l^m(\hat{n}) \exp(i\mathbf{k}\cdot\mathbf{x}), \tag{48}$$

$${}_{\pm 2}G_l^m(\mathbf{k},\mathbf{x},\hat{n}) \equiv (-)^l \sqrt{\frac{4\pi}{2l+1}} {}_{\pm 2}Y_l^m(\hat{n}) \exp(i\mathbf{k}\cdot\mathbf{x}), \tag{49}$$

where the functions $Y_l^m(\hat{n})$ are the standard spherical harmonics and the functions ${}_{\pm 2}Y_l^m(\hat{n})$ are the spin-weighted spherical harmonics [60–62]. Note that the decomposition on the basis $Q_{ij}^{(\pm 2)}$ in the previous section is enlightened by the fact that $Q_{ij}^{(m)} n^i n^j = G_2^{(m)}$ [45,58].

The angular correlation function of these temperature/polarization anisotropies are observed on a two-sphere around us and can be decomposed in Legendre polynomials P_l as

$$\left\langle \frac{\delta U}{T}(\hat{\gamma}_1) \frac{\delta V}{T}(\hat{\gamma}_2) \right\rangle = \frac{1}{4\pi} \sum_l (2l+1) C_l^{UV} P_l(\hat{\gamma}_1 . \hat{\gamma}_2), \tag{50}$$

where U, V stand for Θ, E, or B. Now the brackets stand for an average on the sky, i.e., on all pairs $(\hat{\gamma}_1, \hat{\gamma}_2)$ such that $\hat{\gamma}_1 \cdot \hat{\gamma}_2 = \cos\theta_{12}$. Using the orthonormality properties of the eigenfunctions G, equations (46),(47) can be inverted to extract the angular power spectra C_l^{UV} of the temperature and polarization anisotropies as

$$T_0^2 (2l+1)^2 C_l^{UV}(\eta_0) = \frac{2}{\pi} \int \frac{dk}{k} \sum_{m=\pm 2} k^3 U_l^{(m)}(\eta_0,k) \times V_l^{(m)*}(\eta_0,k). \tag{51}$$

The equations of evolution of the temperature and polarization multipoles $\Theta_l^{(m)}$, $E_l^{(m)}$, and $B_l^{(m)}$ can be obtained by decomposing the Boltzmann equation satisfied by the photon (or neutrino) distribution function on the eigenfunctions G to get

$$\dot{\Theta}_l^{(m)} = k\left[\frac{{}_0\kappa_l^m}{2l-1} \Theta_{l-1}^{(m)} - \frac{{}_0\kappa_{l+1}^m}{2l+3} \Theta_{l+1}^{(m)} \right] - \dot{\tau}\Theta_l^{(m)} + \delta_{l,2} S^{(m)}, \tag{52}$$

$$\dot{E}_l^{(m)} = k\left[\frac{{}_2\kappa_l^m}{2l-1} E_{l-1}^{(m)} - \frac{2m}{l(l+1)} B_l^{(m)} - \frac{{}_2\kappa_{l+1}^m}{2l+3} E_{l+1}^{(m)} \right] - \dot{\tau}(E_l^{(m)} + \delta_{l,2}\sqrt{6} P^{(m)}), \tag{53}$$

$$\dot{B}_l^{(m)} = k\left[\frac{{}_2\kappa_l^m}{2l-1} B_{l-1}^{(m)} + \frac{2m}{l(l+1)} E_l^{(m)} - \frac{{}_2\kappa_{l+1}^m}{2l+3} B_{l+1}^{(m)} \right] - \dot{\tau} B_l^{(m)}, \tag{54}$$

where

$$S^{(m)} \equiv \dot{\tau} P^{(m)} - \dot{H}^{(m)}, \tag{55}$$

$$P^{(m)} \equiv \frac{1}{10}(\Theta_2^{(m)} - \sqrt{6} E_2^{(m)}), \tag{56}$$

$${}_s\kappa_l^m \equiv l\sqrt{\left(1 - \frac{m^2}{l^2}\right)\left(1 - \frac{s^2}{l^2}\right)}. \tag{57}$$

The differential optical depth $\dot{\tau}$ vanishes for neutrinos (except in the very early universe, but the observable wavelengths in the CMB are not affected by this) and is proportional to the free electron density in the case of photons. It has to be calculated by solving the relevant kinetic recombination equations for hydrogen and helium [63–65].

The quantity $P^{(m)}$ represents the coupling between temperature and polarization. Due to our choice of decomposition, only the electric part of the polarization is affected by temperature anisotropies. However, electric and magnetic part of polarization couple themselves as photons propagate. The Clebsch-Gordan coefficients ${}_s\kappa_l^m$ arise from product properties of spherical harmonics. They are obtained in the same way as for the scalar modes [65].

$$\frac{\Theta_l^{(m)}(\eta_0,k)}{2l+1} = \int_0^{\eta_0} d\eta e^{-\tau} S^{(m)} j_l^{(m)}(k(\eta_0 - \eta)), \tag{58}$$

$$\frac{E_l^{(m)}(\eta_0,k)}{2l+1} = -\sqrt{6}\int_0^{\eta_0} d\eta\, \dot{\tau} e^{-\tau} P^{(m)} \times \epsilon_l^{(m)}(k(\eta_0 - \eta)), \tag{59}$$

$$\frac{B_l^{(m)}(\eta_0,k)}{2l+1} = -\sqrt{6}\int_0^{\eta_0} d\eta\, \dot{\tau} e^{-\tau} P^{(m)} \times \beta_l^{(m)}(k(\eta_0 - \eta)). \tag{60}$$

The functions $j_l^{(m)}$, $\epsilon_l^{(m)}$ and $\beta_l^{(m)}$ are defined in terms of the spherical Bessel functions, $j_l(x)$ as

$$j_l^{(\pm 2)}(x) \equiv \sqrt{\frac{3}{8}\frac{(l+2)!}{(l-2)!}}\frac{j_l(x)}{x^2}, \tag{61}$$

$$\epsilon_l^{(\pm 2)}(x) \equiv \frac{1}{4}\left[-j_l(x) + j_l''(x) + 2\frac{j_l(x)}{x^2} + 4\frac{j_l'(x)}{x}\right], \tag{62}$$

$$\beta_l^{(\pm 2)}(x) \equiv \pm\frac{1}{2}\left[j_l'(x) + 2\frac{j_l(x)}{x}\right] \tag{63}$$

where a prime denotes a derivative with respect to the argument x.

Beside the small contribution due to the polarization in Eq. (58), the temperature fluctuation in the direction $\hat{\gamma}$ reduce to the well known result by Sachs and Wolfe [59]

$$\frac{\delta T}{T}(\hat{\gamma}) = -\frac{1}{2}\int_{\eta_{\rm LSS}}^{\eta_0} \dot{h}_{ij}\gamma^i\gamma^j d\eta, \tag{64}$$

where the subscript LSS stands for last scattering surface. The ''visibility function'' $\dot{\tau}e^{-\tau}$ appearing in equations (59),(60) takes a nonzero value only at the time of decoupling so that, contrarily to temperature anisotropies which are constantly generated by gravitational interactions with photons, polarization is generated only at the last scattering surface.

IV. DAMPING OF THE GRAVITATIONAL WAVES

We first study the effect of the damping of the gravitational waves due to the anisotropic stress of the photons. Such a damping of the amplitude of gravitational waves in various viscous cosmic media has been already discussed in Ref. [73]; we give a description of this damping in the formalism we use here in order to quantify precisely its effect on CMB anisotropies. On subhorizon scales larger than the diffusion length $\lambda_{\rm D} \equiv \dot{\tau}^{-1}$ of the photons, i.e., such that

$$\mathcal{H}_{\rm eff} \equiv \tau_{\mathcal{H}}^{-1} \ll k \ll \dot{\tau}, \tag{65}$$

the set of equations (52)–(57) implies that

$$\Theta_2^{(\pm 2)} = -\frac{4}{3}\frac{\dot{H}}{\dot{\tau}} \quad \text{and} \quad E_2^{(\pm 2)} = -\frac{\sqrt{6}}{4}\Theta_2^{(\pm 2)}. \tag{66}$$

Since $\pi^{(\pm 2)}$ is proportional to $\Theta_2^{(\pm 2)}$, we can insert the former expressions in the gravitational waves evolution equation (41) to get the back reaction of the anisotropic stress

$$\ddot{H} + 2\mathcal{H}_{\rm eff}\dot{H} + k^2 H = -\frac{32}{15}\kappa P a^2 \frac{\dot{H}}{\dot{\tau}}. \tag{67}$$

Setting

$$H \equiv \overline{H} h, \tag{68}$$

with $\overline{H}$ solution of the homogeneous equation of evolution (i.e., with $\pi^{(m)}=0$), we get

$$\overline{H}\ddot{h} + \left(2\dot{\overline{H}} + 2\mathcal{H}_{\rm eff}\overline{H} + \frac{32}{15}\kappa P a^2 \frac{\dot{\overline{H}}}{\dot{\tau}}\right)\dot{h} + \frac{32}{15}\kappa P a^2 \frac{\dot{\overline{H}}}{\dot{\tau}} h = 0. \tag{69}$$

Now, (i) since $\dot{\overline{H}} \simeq k\overline{H}$, we deduce that $\dot{\overline{H}} \gg \mathcal{H}_{\rm eff}\overline{H}$, (ii) since $\kappa P a^2 \simeq \mathcal{H}_{\rm eff}$, it follows that $(32/15)\kappa P a^2 \dot{\overline{H}}/\dot{\tau} \simeq \mathcal{H}_{\rm eff}^2/\dot{\tau} \ll k\overline{H} \simeq \dot{\overline{H}}$, and (iii) since $\ddot{h} \simeq \dot{h}/\tau_{\rm D}$, $\overline{H}\ddot{h} \ll \dot{\overline{H}}\dot{h}$ and in conclusion in the limit (65) the equation of evolution of the gravitational waves in presence of the anisotropic stress (69) reduces to

$$\dot{h} = -\frac{16}{15}\kappa P a^2 \dot{\tau} h. \tag{70}$$

We deduce that a mode k is damped from the time it enters the Hubble radius, i.e., $\eta \simeq k^{-1}$ since it happens during the radiation era, to roughly the time when the anisotropic stress becomes negligible, i.e., approximately at the time of last scattering $\eta_{\rm LSS}$. It follows that

$$h(k,\eta_{\rm LSS}) \simeq \exp\left(-\frac{16}{15}\int_{1/k}^{\eta_{\rm LSS}} \frac{\kappa P a^2}{\dot{\tau}} d\eta\right) h(k,1/k). \tag{71}$$

This damping of the gravitational waves by the anisotropic stress of the photon fluid is analogous to the damping of the scalar modes (density fluctuations) known as the Silk damping [74] a description of which, in the formalism used here, can be found in Ref. [58]. Note however that the origin of the damping is different.

This effect is small but, apart from Ref. [73], was not much emphasized in the literature before. Assuming that the universe is completely ionized until the last scattering surface, the integral of Eq. (71) is of order [75]

$$\frac{1}{3}\left(1 - \frac{Y_{\rm He}}{2}\right)\frac{\Omega_\gamma^0}{\Omega_b^0}\frac{m_{\rm p}\kappa}{\sigma_{\rm Th}} a_0(\eta_{\rm LSS} - 1/k) \simeq 10^{-3}(1 - 1/k\,\eta_{\rm LSS}), \tag{72}$$

where $m_{\rm p}$ is the proton mass, $\sigma_{\rm Th}$ is Thomson scattering cross section. The real damping factor is greater than the estimate (72) because the universe becomes neutral at the last scattering surface (so that the term $\dot{\tau}$ is smaller). In Fig. 1 (left), we plot this damping factor for the modes that entered into the Hubble radius long before the last scattering surface (i.e., such that $k \gg \eta_{\rm LSS}^{-1}$). As a consequence, the comparison between the damped case to the undamped case, shozn on Fig. 1 (right) does not show significant differences. The amplitude of the high-l tail of the CMB anisotropy spectrum is lowered by roughly 10% when one includes this effect. The same occurs of course for polarization. We emphasize that this result does not depend on any particular model, and is not included in the most recent (3.2) version of CMBFAST.

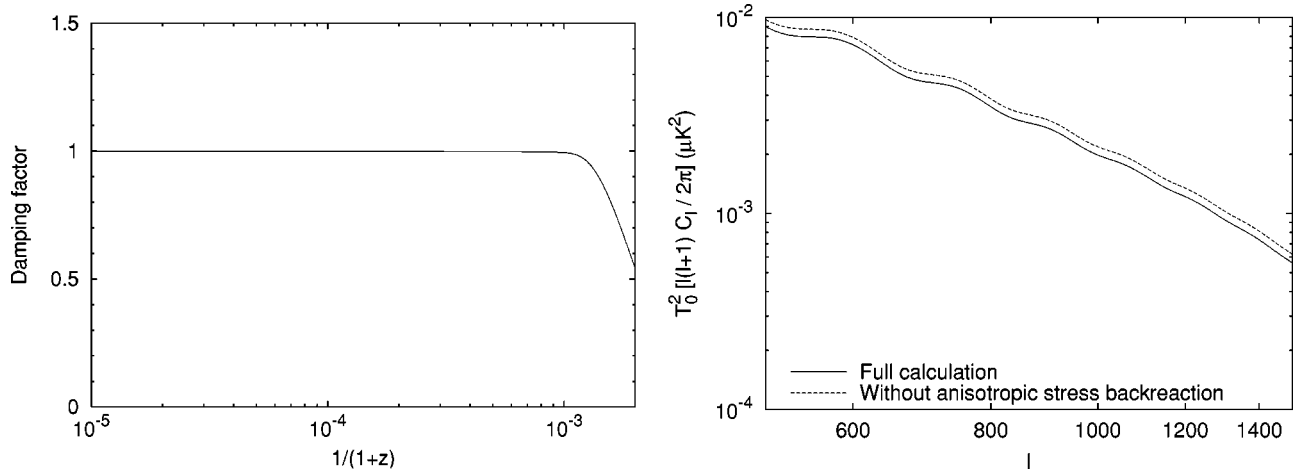

FIG. 1. Damping of the gravitational waves due to its coupling to the photons anisotropic stress. The damping (left figure) is generated only when the universe becomes neutral, i.e., soon before the last scattering surface. As a consequence, all the mode which have already entered into the Hubble radius at recombination are equally damped, regardless of their wavelength. The influence of this damping on the CMB anisotropies is shown on the right figure. Since all the modes are equally damped, this translates into a constant ratio of amplitude between the damped and the undamped cases. Note, however, that our derivation is valid only when Eq. (65) applies, which is not true at the end of decouling, when $\dot{\tau}$ becomes small. This is why the actual damping (10%) is smaller than what is expected from the left plot.

V. SPECIFICATION OF THE MODEL

A. Model parameters

At this stage, the model we are discussing depends on five parameters: (1) $f(\phi)$ which is an arbitrary function of the scalar field ϕ, (2) ξ the coupling of the scalar field with the background spacetime, (3) α the slope of the potential (14) or (16), (4) Ω_ϕ^0 the energy density in the scalar field today, and (5) $P_T(k)$ the spectrum of the gravitational waves.

Indeed there exist some constraints on these functions and parameters and we make the following assumptions and choices.

(1) We assume that $f(\phi)=\phi^2/2$; this is the only choice for which the coupling constant ξ is dimensionless. Moreover such a choice can be seen as the lowest term in an expansion of f in powers of ϕ. As shown in Ref. [22] there exists tracking solutions for the field ϕ evolving in the potential (14) with such a coupling.

(2) If the scalar field ϕ is coupled to the spacetime metric, this coupling must be weak enough so that it does not generate a significant time variation of the constants of nature [29]. Taking into account the bound on the variation $|\dot{G}/G|$ of the Newton constant [66] and on the variation $|\dot{\alpha}/\alpha|$ of the fine structure constant [67], it was shown [30] that

$$-10^{-2}\lesssim\xi\lesssim 10^{-2}-10^{-1}. \tag{73}$$

This bound is, however, sensitive to the shape of the potential. On the other hand the experimental constraints (from the Shapiro effect and the light deflection in the Solar system) on the post-Newtonian parameters [57,68] imply [30]

$$|\xi|\lesssim\frac{3.9\times 10^{-2}}{\sqrt{\alpha(\alpha+2)}}. \tag{74}$$

However, in this class of models one does not try to have a theory converging towards general relativity at late time and the coupling ξ is constant which is the main reasons of the severe bounds on its value. This can be improved by generalizing this kind of models by considering them in the framework of scalar-tensor theories [31,32].

(3) In most models α is not constrained theoretically. If the matter content of the universe today is dominated by the matter-radiation fluid then the fact that the observations [9] favor $-1<\omega_\phi<-0.6$ gives a bound on α, which is indeeed not the case anymore if the scalar field starts to dominate. In Fig. 2 [left], we compare this analytic estimate and the numerical determination of the energy scale Λ as a function of the slope α. We see that if $\alpha>4$ then Λ is at least larger than 1 TeV (when $\Omega_\phi^0=0.7$).

(4) The density parameter Ω_ϕ^0 is not severely constrained theoretically, but observations seem to indicate $\Omega_\phi^0\simeq 0.7$. One has to check that if the scalar field was dominating the matter content of the universe at some early stage then it has to be subdominant at the time of nucleosynthesis (see, e.g., Ref. [69]). The choice of Ω_ϕ^0 fixes the value of the energy scale Λ in Eq. (14) or (16); this is the *coincidence problem*. On Fig. 2 (right), we depict the variation of the energy scale Λ with Ω_ϕ^0 and α. It is not very sensitive to Ω_ϕ^0 as long as $0.1<\Omega_\phi^0<0.9$. In fact, when the quintessence field starts to dominate the matter content and if we have reached the attractor then $d^2V/d\phi^2\propto H^2$ (see Ref. [18]), and $H^2\simeq V/M_{\rm Pl}^2$ so that we can estimate that the variation of Λ with α follows

$$\Lambda=(\rho_{\rm crit}M_{\rm Pl}^{\alpha})^{1/(4+\alpha)}. \tag{75}$$

We conclude that

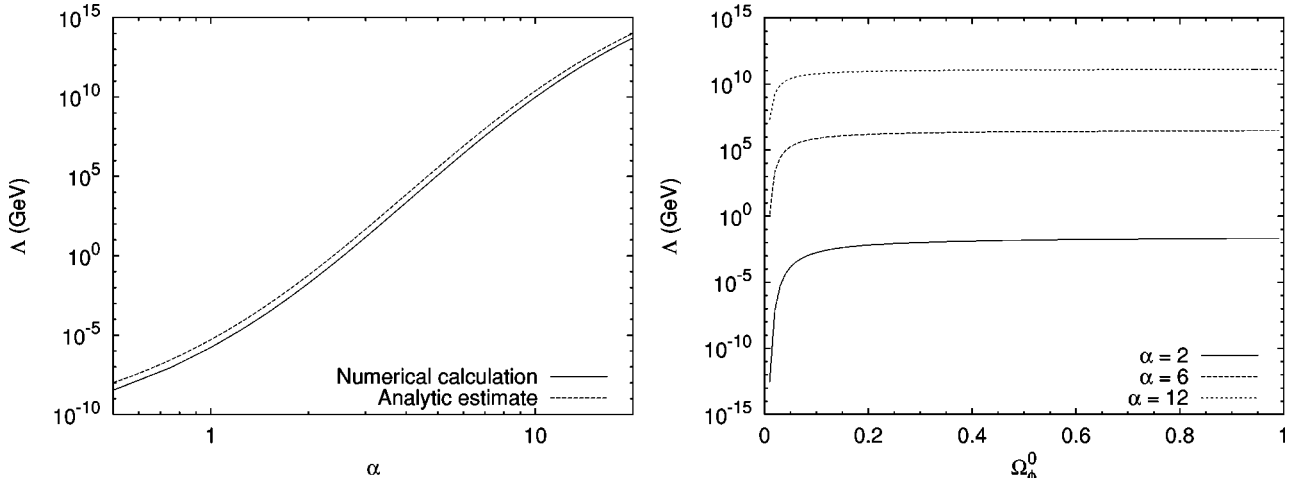

FIG. 2. Variation of the energy scale Λ of the potential (14) with the energy density of the scalar field Ω_ϕ^0 and the slope of the potential α. We first show (left) the variation of Λ with α when $\Omega_\phi^0=0.7$ and the comparison with the analytic estimate (75) and (right) the variation of Λ with Ω_ϕ^0 for $\alpha=2,6,12$.

$$\frac{\delta\Lambda}{\Lambda}\sim\frac{1}{4+\alpha}\frac{\delta\Omega_\phi^0}{\Omega_\phi^0}$$

and thus a prescision of 10% on Ω_ϕ^0 requires to tune Λ at a 1% level if e.g. $\alpha=6$, which is a less drastic tuning than the usual cosmological constant fine tuning problem.

(5) P_T has to be determined by a specific model, such as, e.g., inflation, and we parametrize it as

$$P_T(k)\equiv A_T k^{n_T} \tag{76}$$

where A_T is a constant dans n_T is the tensor mode spectral index. A_T is obtained by normalizing the CMB temperature anisotropies to the Cosmic Background Explorer (COBE) data at $l=10$ for which

$$T_0\sqrt{\frac{l(l+1)}{2\pi}C_l^{\Theta\Theta}}\simeq 30\ \ \mu\mathrm{K}. \tag{77}$$

Since some measurements tend to show that there is a peak at the degree scale [4], we conclude that a significant part of the anisotropies may be generated by the scalar modes. In the ''standard'' slow-roll inflation picture, this is compatible with an almost scale-invariant spectrum with a low tensor contribution, in which case the COBE results would put only an upper limit on the amplitude of the gravitational waves spectrum. Nevertheless, we point out that it is also possible that most of the large scale anisotropies can be generated by gravitational waves. This assumes a strong deviation from scale invariance ($n_S=1.69$ and $n_T=0.0$), but is in good agreement with observational data [70].

B. Initial conditions and behavior of the background spacetime

Concerning the initial conditions for the scalar field ϕ, we will consider the two extreme cases: (IC1) where we assume that the scalar field is at equipartition with the matter (i.e., mainly with the radiation) deep in the radiation era and (IC2) where it dominates the matter content of the universe at a very early stage. Situation (IC1) implies that at the end of reheating

$$\rho_\phi\lesssim 10^{-4}\rho_\gamma, \tag{78}$$

where the factor 10^{-4} is roughly the inverse of the number of degrees of freedom at that time. Since the quintessence field is already subdominant at this epoch, one does not need to care about its effect on nucleosynthesis since it remains subdominant until recently. In the second situation (IC2), the field starts by dominating and inflation ends by a kinetic phase rapidly than ρ_γ and will thus become subdominant. One has to check that this happens before nucleosynthesis [46,48]. A realization of such initial conditions can be obtained in quintessential inflation [48].

In Fig. 3, we depict the evolution of the energy density of the quintessence field, matter and radiation for the initial conditions (IC1) (left) and (IC2) (right). We see that for a very large range of initial conditions (roughly for $10^{-47}\ \mathrm{GeV}^4\lesssim\rho_\phi\lesssim 10^{113}\ \mathrm{GeV}^4$ at a redshift of $z\simeq 10^{30}$) we end up with a quintessence field which starts to dominate today. This explains briefly how the fine tuning problem is solved [21]. We can also check that with these values the scalar field does not dominate the matter content of the universe at nucleosynthesis, i.e., at a redshift of order $z\simeq 10^{10}$.

An interesting point concerns the evolution of the scalar field equation of state in the case (IC2) when $\xi=0$. The field rolls down very fastly so that we are first in a regime where

$$\rho\simeq P\simeq\frac{1}{2}\frac{\dot\phi^2}{a^2} \tag{79}$$

from which we conclude that its equation of state is $\omega_\phi\simeq 1$ (see Fig. 4). But, because of the exponential behavior contribution of the potential, the field is stopped when $\phi\gtrsim M_{\mathrm{Pl}}$ and then rolls back to smaller values (see Fig. 5) so that the field undergoes a series of damped oscillations (because of the friction term coming from the expansion in the Klein-

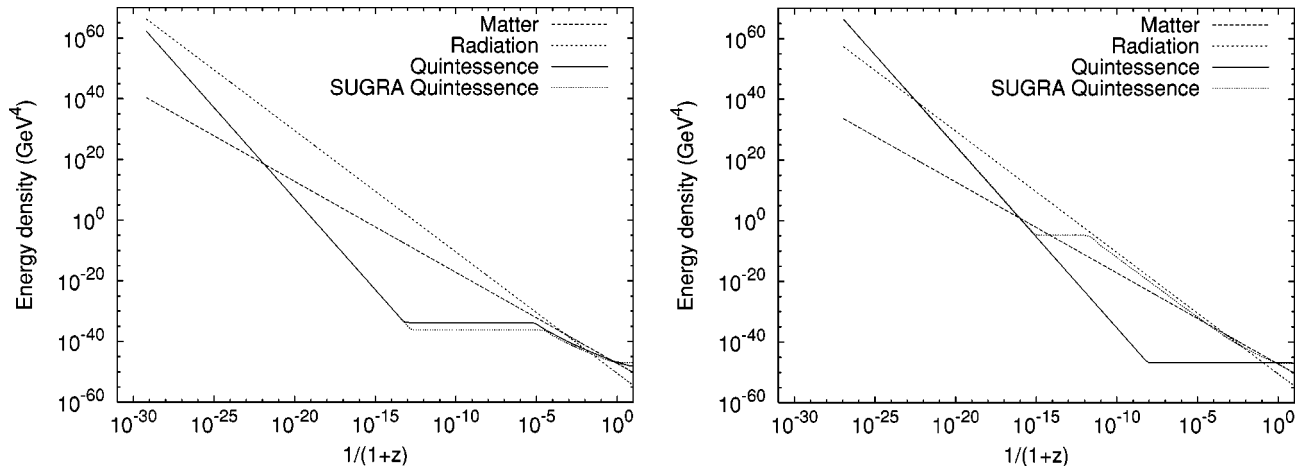

FIG. 3. The behavior of the energy density of the matter (long-dashed line), radiation (short-dashed line), and scalar field (solid and dotted lines), as a function of the redshift for the two class of initial conditions: (IC1), when the field is at equipartition with the radiation (left), and (IC2), when the field initially dominates the matter content of the universe (right). The solid line represents the case when the field evolves in an inverse power-law potential, and the dotted line represents the case when the field evolves in the supergravity (SUGRA) potential. Note that when the field dominates at early times, the SUGRA potential stabilizes the field, which reaches the tracking solution earlier.

Gordon equation). This implies that there exist times such that $\dot{\phi}\simeq 0$ and thus small period around them where the equation of state varies rapidly to $\omega_\phi \simeq -1$ (see Fig. 4). This sudden change in the equation of state of ϕ happen while it is dominating the matter content of the universe (see Fig. 3) so that it implies variations in the evolution of the scale factor of the universe which, in principle, should let a signature in the gravitational waves energy spectrum. Indeed, this does not happen in standard quintessence and is a specific feature of the SUGRA quintessence.

When $\xi \neq 0$, there are no significant modifications to the background dynamics as long as the field has not reached the Planck mass [because $2\xi\kappa f(\phi)$ is small compared to unity, see Eq. (5)]. Then, the main difference appears at late times when the field starts to dominate and comes from the fact that the bound $-1<\omega_\phi<1$ no longer applies, and one can get lower values of ω_ϕ. Equivalently, the equation of state parameter $\omega \equiv (P_{\rm fluid}+P_\phi)/(\rho_{\rm fluid}+\rho_\phi)$ for the whole background fluids can reach values smaller than -1 (see Fig. 6 where we plot the variation of ω_ϕ as a function of redshift). As pointed out by Caldwell [10], such a matter fits the current observational data. Different candidates such as a decaying dark matter component [71] and a kinetic quintessence field [72] were proposed. Here, we show that any nonminimally coupled scalar field may be a good candidate for a component of matter with $\omega<-1$. The constraints (73) on ξ implies that for our class of models

$$-3 \leqslant \omega_\phi < 0$$

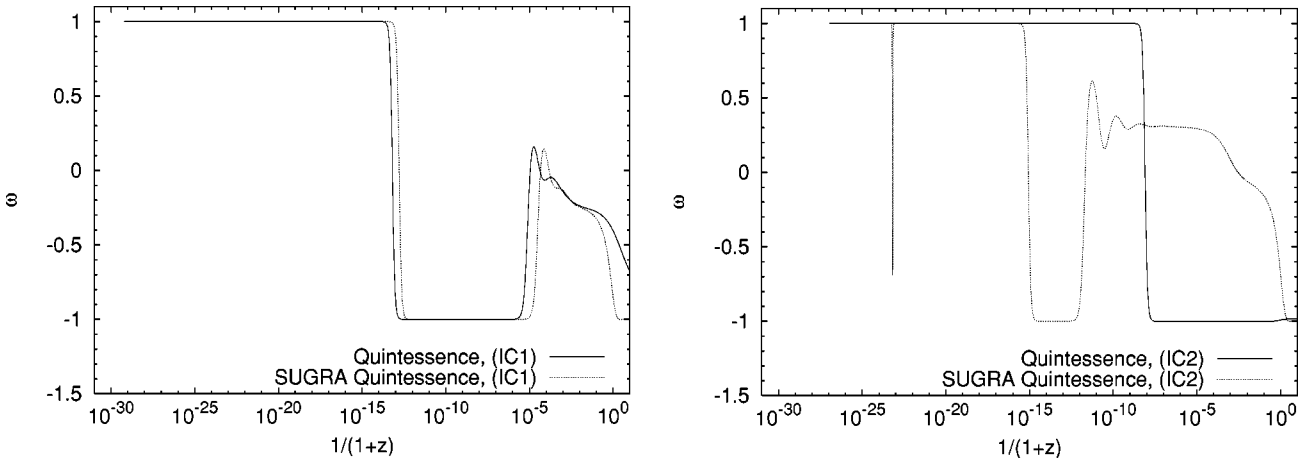

FIG. 4. The behavior of the equation of state parameter as a function of the redshift for the two class of initial conditions: (IC1), when the field is at equipartition with the radiation (left), and (IC2), when the field initially dominates the matter content of the universe (right). The solid line represents the case when the field evolves in an inverse power-law potential, and the dotted line represents the case when the field evolves in the SUGRA potential. In the case of (IC2), the field reaches the tracking solution only when SUGRA corrections to the potential are considered. Note also the spikes in the SUGRA case (right), which illustrate the fact that the field bounces around the Planck scale (see Fig. 5 below).

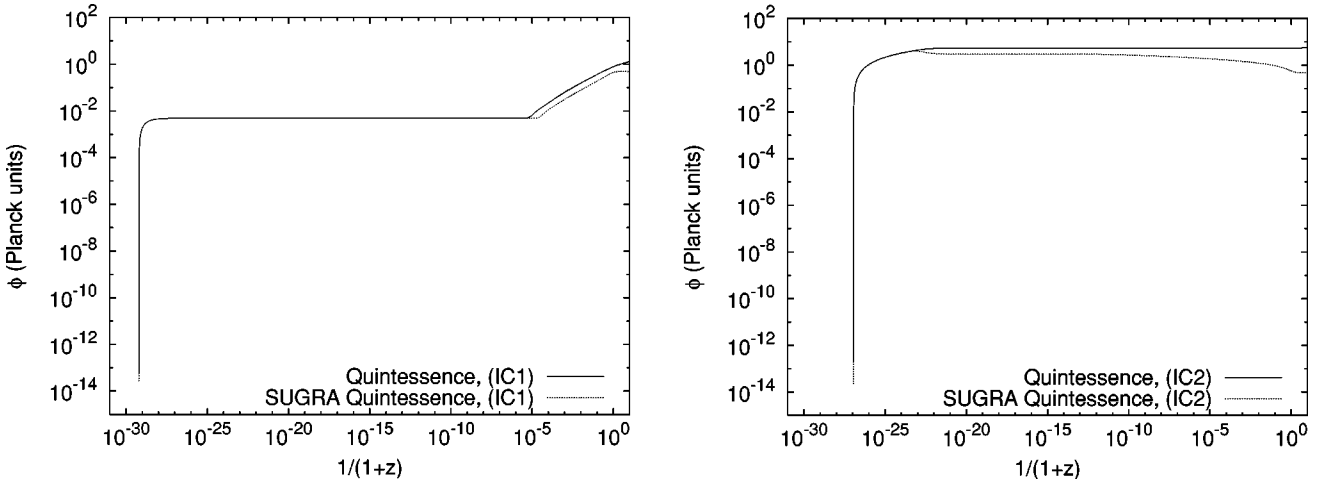

FIG. 5. The behavior of the quintessence field as a function of the redshift for the two class of initial conditions: (IC1), when the field is at equipartition with the radiation (left), and (IC2), when the field initially dominates the matter content of the universe (right). The solid line represents the case when the field evolves in an inverse power-law potential, and the dotted line represents the case when the field evolves in the SUGRA potential. In the case of (IC1), the field always reaches the tracking solution before today, whereas for (IC2), the field reaches the tracking solution only when it evolves in the SUGRA potential.

if the scalar field dominates. We emphasize that ω_ϕ is not uniquely defined according to the way one splits $T^{\mu\nu}_{(\phi)}$ in (6). In Fig. 6, we used the Friedmann equations (7),(8) to extract ω from

$$\frac{\dot{\mathcal{H}}}{\mathcal{H}^2}-1=-\frac{3}{2}(1+\omega)\Omega$$

and then ω_ϕ from

$$\omega\Omega=\sum_i \omega_i\Omega_i,$$

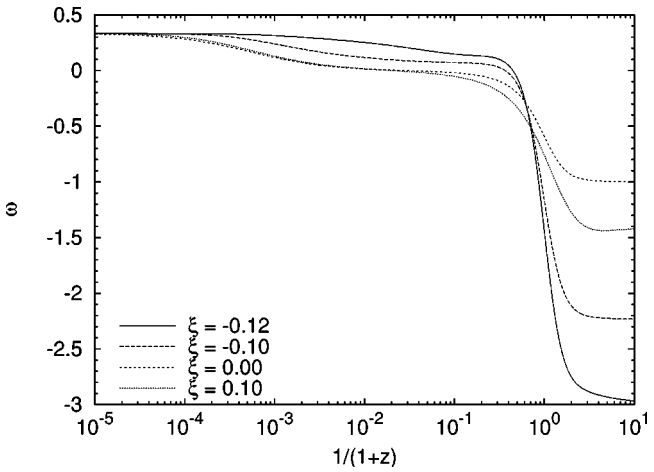

FIG. 6. Evolution of the equation of state parameter ω as a function of the redshift for different values of the coupling ξ. As soon as the coupling is not minimal, ω can reach values smaller than -1. The parameters of the model considered here are: $\alpha=6$, potential (16) including SUGRA corrections, $\Omega^0_\phi=0.7$ and (IC1) initial conditions.

where i runs on all the matter species. This corresponds to the value of ω as it may be reconstructed from observational data such as, e.g., the supernovae type Ia.

VI. QUALITATIVE DISCUSSION

A. Gravitational waves spectrum

Equation (41) describes the evolution of a damped oscillator. Injecting the ansatz

$$H^{(m)}\equiv A^{(m)}\exp(ik\eta) \tag{80}$$

in Eq. (41) and performing a WKB approximation leads to the equation

$$\dot{A}^{(m)}+\mathcal{H}_{\rm eff}A^{(m)}=0 \tag{81}$$

for the evolution of the amplitude $A^{(m)}$ where $\mathcal{H}_{\rm eff}\equiv\dot{\tilde{a}}/\tilde{a}$, with

$$\tilde{a}\equiv a\sqrt{1-2\kappa\xi f(\phi)}. \tag{82}$$

This WKB approximation holds only for ''sub-horizon'' modes. Before a mode has a wavelength smaller than the Hubble radius, its amplitude evolves according to

$$\ddot{A}^{(m)}+2\mathcal{H}_{\rm eff}\dot{A}^{(m)}=0, \tag{83}$$

the solutions of which are a constant mode and a decaying mode. Neglecting the decaying mode, we see that the wave is ''frozen'' as long as its wavelength is larger than the Hubble radius, and that it undergoes damped oscillations once its wavelength is shorter than the Hubble radius. The damping of a mode of wavenumber k between the time it enters the Hubble radius and today is then proportional to

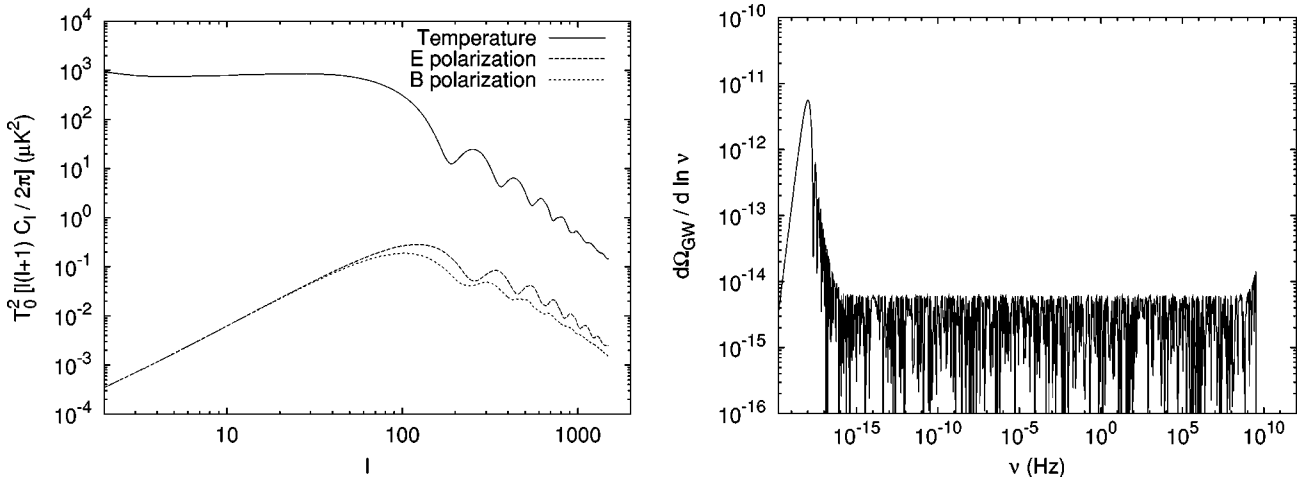

FIG. 7. The temperature et polarization of the CMB induced by gravitational waves (left) and their energy density spectrum (right) in a standard ΛCDM model with $n_T=0$.

$$\frac{\tilde{a}_k}{\tilde{a}_0}, \tag{84}$$

where $\tilde{a}_k$ is the scale factor evaluated at the time η_k when the mode k enters the Hubble radius (i.e., when $\mathcal{H}=k$) and $\tilde{a}_0$ is scale factor today. Injecting this behavior in Eq. (36), we obtain that the energy density spectrum of gravitational waves scales as

$$\frac{d\Omega_{\rm GW}}{d\ln(k)} \propto k^2 \tilde{a}_k^2 P_T(k). \tag{85}$$

First let us assume that $\xi=0$. For wavelengths corresponding to modes that have entered the Hubble radius in the matter dominated era (for which $a \propto \eta^2$ and thus $\eta_k \simeq k^{-1}$), one can easily sort out that

$$\tilde{a}_k \simeq k^{-2} \tag{86}$$

and the gravitational waves spectrum behaves as

$$\frac{d\Omega_{\rm GW}}{d\ln(k)} \propto k^{-2} P_T(k). \tag{87}$$

Equivalently, for wavelengths corresponding to modes entering the Hubble radius in the radiation dominated era (for which $a \propto \eta$) one can show that the gravitational waves energy spectrum behaves as

$$\frac{d\Omega_{\rm GW}}{d\ln(k)} \propto k^0 P_T(k). \tag{88}$$

To finish, if it happens that there exist wavelengths corresponding to modes that have entered the Hubble radius while the scalar field was dominating (for which $a \propto \sqrt{\eta}$ since $\rho_\phi \propto 1/a^6$) one obtains that

$$\frac{d\Omega_{\rm GW}}{d\ln(k)} \propto k^1 P_T(k). \tag{89}$$

In conclusion, we have found three behaviors for the gravitational waves spectrum according to the wavelength. In Fig. 9, we give an example of such a spectrum in a case where one has a scalar field dominating at early stage [initial condition (IC2)]. These results hold also when $\xi \neq 0$ but the slopes of the spectrum are slightly changed since the time behavior of a has to be replaced by the one of $\tilde{a}$.

B. CMB anisotropies

For scales smaller than the Hubble radius at decoupling, one can follow the same lines to predict the tensor part of the CMB temperature anisotropies. The main difference is that the expression for $l(l+1)C_l$ does not involve any factor k^2 as in Eq. (45), the reason being that Eq. (58) can be integrated by parts to drop the time derivative of $H^{(m)}$, which shows that anisotropies are mostly generated on the last scattering surface with an amplitude of $|H^{(m)}|^2$. Therefore, the spectrum behaves as

$$l(l+1)C_l \propto l^{n_T-4}, l^{n_T-2}, l^{n_T-1}, \tag{90}$$

for modes which have entered the Hubble radius is the matter dominated, radiation dominated and kinetic scalar field dominated eras respectively. With standard cosmological parameters, the radiation to matter transition occurs soon before the decoupling, and the scalar field dominates only at very early times. As a consequence, one sees almost only the regime $l(l+1)C_l \propto l^{n_T-2}$. For modes which enter into the Hubble radius after the last scattering surface, one can show [44] that the produced spectrum scales as

$$l(l+1)C_l \propto l^{n_T}. \tag{91}$$

Note that this expression is indeed an approximation and that it is not easy to calculate an accurate analytical solution [76]. These results are illustrated in Fig. 7. As already stressed, the result of Eq. (91) applies at large angular scales which have not entered into the Hubble radius at recombination. For standard cosmologies, this occurs for multipoles smaller than $l \simeq 100$ (in addition, there are also some corrections to this

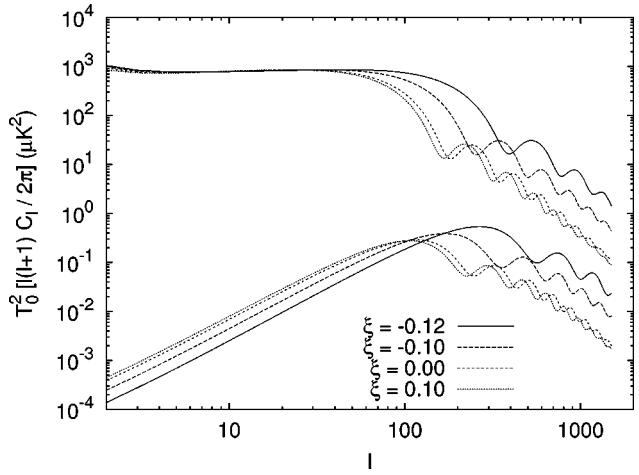

FIG. 8. Influence of the coupling ξ on the CMB temperature and polarization anisotropies. The value of ξ influences the angular diameter-distance relation and therefore affects the overall position of the spectrum. The parameters of the model considered here are the same as in Fig. 6: $\alpha=6$, potential (16) including SUGRA corrections, $\Omega_\phi^0=0.7$ and $n_T=0$.

rough estimate which occur at the very smallest multipoles and slightly boost the spectrum, as can also be seen on Fig. 7). Then, at higher multipoles the result of Eq. (90) is valid. The matter dominated regime before recombination is rather short, and occurs only between $l\simeq 100$ and $l\simeq 200$ (less than one oscillation in the spectrum). For $l\gtrsim 200$, one sees the regime $l(l+1)C_l\propto l^{n_T-2}$ (see also Fig. 1 of Ref. [44]).

C. Results of the ΛCDM model

Before turning to a more general numerical study of the class of models we consider in this article, we recall in Fig. 7 the general results for the temperature and polarization angular power spectra and the gravitational waves density spectrum for a ΛCDM model. This spectrum has two branches: a soft branch at lower frequencies (corresponding to the matter dominated era) and a hard branch at higher frequencies (corresponding to modes that entered the horizon in the radiation era). Following Ref. [34], we set the cutoff on this spectrum to the last mode that has been inflated out of the Hubble radius.

VII. NUMERICAL RESULTS

A. Field ϕ initially at equipartition

Since the scalar field only starts to dominate at very recent time, we expect no effect on the gravitational waves energy spectrum (since at earlier time the universe is always radiation dominated). However, the change in today's universe equation of state yield a specific signature in the angular diameter-distance relation. Hence, one expects to see the quintessence field behavior in the positions of the peaks in the CMB anisotropy spectra.

The temperature anisotropies plots of Fig. 8 are therefore identical at high multipoles except for their overall position which are different. At low redshift, the scalar field dominates and the dynamics of the expansion depends explicitely of the value of the coupling ξ, which cause some slight differences in the CMB anisotropies at the very first multipoles ($l\leqslant 5$). We have also seen that the polarization is generated by gravity and therefore different gravitational constants lead to different normalization between the polarization and the temperature spectra. Since we normalize the ''bare'' Einstein constant κ so that the effective Einstein constant corresponds to what we measure (in e.g. a Cavendish experiment), models with a different ξ have different κ. At decoupling, the scalar field does not dominate and therefore $\kappa^{\rm LSS}=\kappa_{\rm eff}^{\rm LSS}$. This induces different amplitudes for the polarization anisotropy spectra. For the lowest values of ξ there is a factor 2 -4 in amplitude as compared with the $\xi=0$ case, which roughly corresponds to the square of the variation of $\kappa_{\rm eff}$ (and, hence G) between the last scattering surface and now. Note that the effect of ξ depends on its sign. This is the reason why the constraint derived by Chiba [30] are stronger for negative values of ξ. The same can be seen in Fig. 6.

We conclude that the temperature anisotropies and polarization give mainly information on the spectral index n_T, the energy density of the scalar field today Ω_ϕ^0 and its coupling ξ.

B. Field ϕ dominates at early stage

We now turn to the more unusual case where the scalar field dominates at the end of inflation and where the universe undergoes a kinetic phase before the radiation era [24,49] as in, e.g., quintessential inflation [48]. The wavelengths corresponding to the observable CMB multipoles ($l\lesssim 2000$) are much larger than the Hubble radius at nucleosynthesis, epoch at which we have to be radiation dominated. As a consequence, we expect no signature from this early phase on the CMB anisotropies and polarization.

As first pointed out in Refs. [46,48], if the scalar field dominates at early stage, there is an excess of gravitational waves at high frequency [see equation (89)]. On Fig. 9, we present such a spectrum and we will discuss the implication of this excess later.

An interesting effect concerns the difference between the spectra obtained from an inverse power law potential and a SUGRA-like potential. As shown on Fig. 9 [right], the amplitude of the spectrum at high frequency in roughly 30% higher for inverse power law potentials. The relative decrease in amplitude at these frequencies for SUGRA-like potentials depends on the dynamics of the scalar field in the bounce (see Figs. 4 and 5) during which the equation of state varies from $+1$ to -1 and to $+1$ again. Thus, during this time, the modes that had just entered into the Hubble radius (and thus which had just started to undergo damped oscillations) went out of it (during the $\omega<0$ epoch) and their amplitude was frozen before reentering the Hubble radius again. Hence, the modes of larger wavelengths are less damped which explains this decrease in amplitude. Now, if the slope of the potential is less steep, the bounce lasts longer (note that we always reach $\omega=-1$ at the point where $\dot\phi=0$) and thus the damping is stronger. This signature, even if not detectable by coming experiment is nevertheless a clear feature of supergravity.

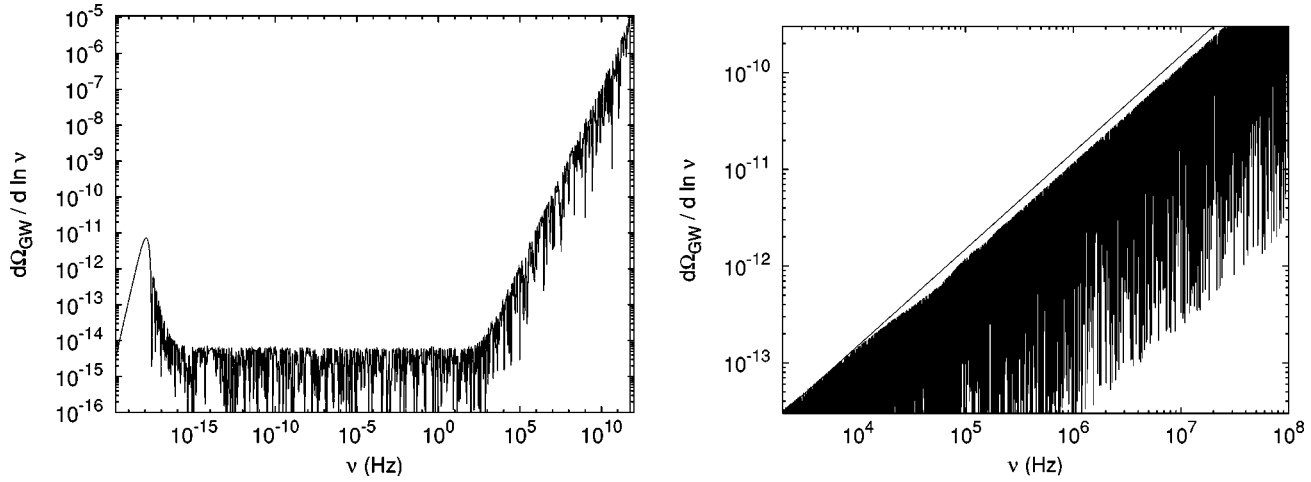

FIG. 9. Gravitational waves spectrum in a quintessence model with (IC2) initial conditions with a SUGRA-like potential. The spectrum has been normalized to be compatible with COBE at large scales. The spike in the evolution of the equation of state of the scalar field (see Fig. 4) yields to a loss (right) of about 20% in the amplitude of the spectrum at high frequency (i.e., $>10^4$ Hz).

To finish, let us discuss the total energy density of gravitational waves $\Omega^0_{\rm GW}$ today. As pointed out in Ref. [46], it has also to be negligible at nucleosynthesis; this constraint is more drastic than the only requirement that Ω^0_ϕ be negligible at that time. Let us emphasize that the constraint on Ω^0_ϕ cannot be avoided (since it involves background dynamics) whereas the one on $\Omega^0_{\rm GW}$ depends on A_T and n_T and thus leads to a combined constraint on the initial conditions of the scalar field and on the initial power spectrum of the gravitational waves. In addition to A_T and n_T, $\Omega^0_{\rm GW}$ mainly depends on the initial values of ρ_ϕ and $\rho_{\rm rad}$ which can be parametrized by the reheating temperature T_R (related roughly to $\rho_{\rm rad}$ at that time) and the redshift z_* of equality between the kinetic scalar field era and the radiation era (related roughly to $\rho_\phi/\rho_{\rm rad}$ at the end of reheating). $\Omega^0_{\rm GW}$ can be estimated by the surface of the spectrum below the part with a positive slope (i.e., the high frequency part; see Fig. 9) and thus of order

$$\Omega^0_{\rm GW} \sim \frac{k_R}{k_*}\left.\frac{d\Omega_{\rm GW}}{d\ln k}\right|_{k_*}, \tag{92}$$

where k_R and k_* are, respectively, the modes entering the Hubble radius at the reheating and at z_*. Thus the ''bump'' at short wavelength cannot be too high. Moreover, the energy density at the end of reheating cannot be higher that Planck scale, so that it fixes a limit on the shortest mode in which gravitational waves are produced. On Fig. 10, we first

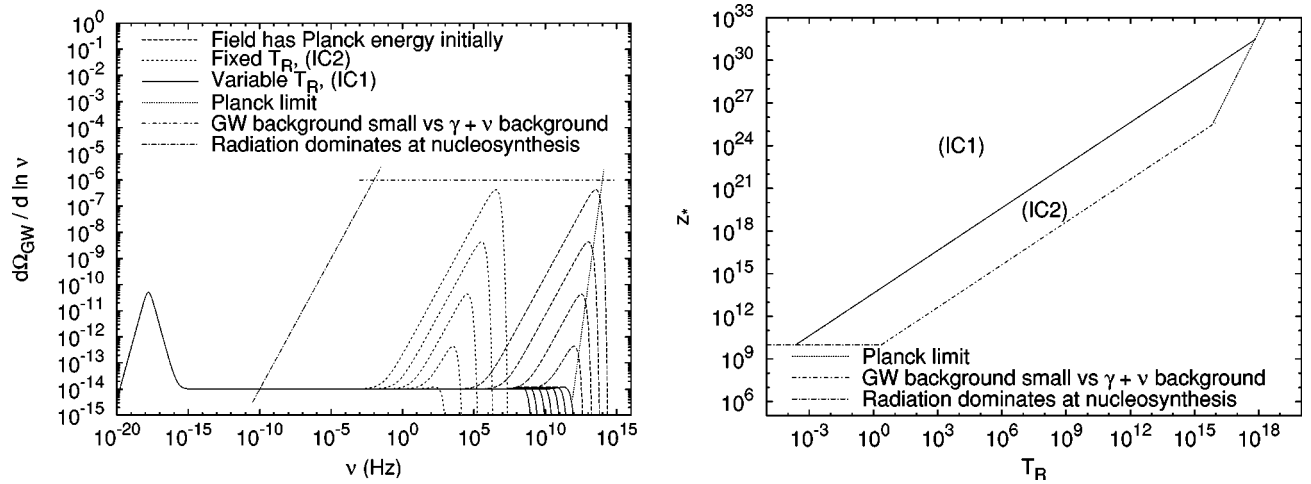

FIG. 10. Variation of the gravitational waves spectrum with the cutoff and with the epoch of transition between scalar field in kinetic regime and radiation (left) and contour plot (right) of the safe zone for nucleosynthesis for the parameter set (T_R, z_*) (above the dotted and dot-dashed lines). Both plots are for a spectral index $n_T=0$ and for maximum A_T allowed by COBE measurements. The solid line is obtained by imposing that the scalar field dominates at the end of inflation: points lying on or above this line have a corresponding solid power spectrum on the left plot. The horizontal dot-dash line is obtained by imposing that we are radiation dominated at nucleosynthesis (i.e., $z_*>10^{10}$). The diagonal dotted line is obtained by imposing that the energy density at the end of inflation is smaller than the Planck density. The diagonal dot-dashed line (''GW background . . . '') is obtained by imposing that $\Omega^0_{\rm GW}<10^{-6}$.

plot [left] the variation of the gravitational wave spectrum with the parameters (T_R, z_*) and we then give [right] the ''safe'' zone of parameters for nucleosynthesis [for $n_T=0$] and defined [46,48] by $\Omega^0_{\rm GW}\lesssim 10^{-6}$. Let us briefly explain how this bounds are obtained.

(1) We first rephrase in terms of T_R the fact that the field is dominating at the end of the inflation phase, i.e.,

$$z_*<z_R \Leftrightarrow z_*<\alpha_1 T_R, \tag{93}$$

where α_1 is some numerical coefficient. This corresponds to the solid line on Fig. 10.

(2) We then impose that the scalar field is subdominant at nucleosynthesis, i.e., that

$$z_*>10^{10}. \tag{94}$$

This corresponds to the horizontal dash-dot line on Fig. 10.

(3) At the end of the inflation phase, we want the energy density to be smaller that the Planck energy density. If the scalar field is dominating if gives

$$\rho^0_\phi \frac{(1+z_R)^6}{(1+z_*)^2}(1+z_{\rm eq})<\rho_{\rm Pl} \Leftrightarrow z_*>\alpha_2 T_R^3, \tag{95}$$

where α_2 is another numerical coefficient. This corresponds to the dot line on Fig. 10. Note that since we are in a field dominated era $H^2\propto a^2$ and thus on this ''Planck limit'' we have $k_R\propto z_R^2/z_*$ and $k_*\propto z_*$ (and thus $k_R\propto 1/z_R$ and $k_*\propto z_R^3$) from which we conclude that the maximum of the power spectrum is roughly located on a curve $(1/z_R, 1/z_R^4)$ (see Fig. 10).

(4) To finish, we want that the gravitational waves energy density does not alter nucleosynthesis, i.e., that

$$\Omega^0_{\rm GW}\lesssim 10^{-6} \Leftrightarrow T_R<\alpha_3 z_*, \tag{96}$$

where α_3 is a third numerical coefficient. This corresponds to the dot-dash line on Fig. 10.

For all the points (T_R, z_*) above the dotted and dot-dashed lines of Fig. 10 (right), there is no excess of gravitational waves. The solid line separates the two sets of initial conditions we have considered. We must emphasize that this result was obtained for $n_T=0$ and that the spectrum can be tilted, which modifies the bounds on the parameter set (T_R, z_*) (more precisely, taking smaller A_T or negative n_T lowers the diagonal dot-dashed line). Such constraints may be important for instance while considering models where a scalar field dominates at baryogenesis [77].

In the case of a ''blue'' initial power spectrum (i.e., with $n_T>0$ in our notations, or $\beta>-2$ in the notations of Ref. [78]), as advocated for example in Ref. [78], the flat branch of Fig. 9 (corresponding to the ''semihard'' branch of Ref. [47]) is already tilted, giving as stronger constraint on our model. For instance, if $n_T=0.2$, the amplitude at $\nu=10$ GHz is boosted by a factor $\simeq 3\times 10^5$. As a consequence, the quantity of gravitational waves at high frequency cannot be boosted as much as in the case of a scale invariant spectrum, and the allowed range of parameters for our model (see Fig. 10) is narrowed.

VIII. CONCLUSION

In this article, we have studied some properties of quintessence models with a nonminimally coupled scalar field among which the spectrum of gravitational waves. We have shown that such a quintessence field can behave as a fluid with $\omega<-1$ and our models lead to $-3\lesssim\omega\lesssim 0$ when the field dominates. We related the energy scale Λ of the potential to its slope α and to the scalar field energy density today Ω^0_ϕ. In particular, we showed that Λ is almost independent of Ω^0_ϕ. The coincidence problem, i.e., the fact that $\Omega^0_\phi\sim 1$ implies a tuning of Λ (roughly the precision on Λ has to one order of magnitude higher than the one on Ω^0_ϕ) which is, however, less severe than the fine tuning needed for a cosmological constant. This being fixed, the tracking mechanism allows to span a very wide range of initial conditions for the scalar field and there is no fine tuning in that respect.

We then showed that the combined study of the gravitational waves energy spectrum and of their imprint on the CMB radiation temperature and polarization enables to extract many complementary informations on the models: the CMB mainly gives results on ξ, Ω^0_ϕ and n_T; the energy spectrum gives results on the initial conditions of the scalar field. As pointed out in Refs. [46,48], there is an excess of gravitational waves today if inflation ends by a kinetic phase. In that case, one has to check that both Ω_ϕ and $\Omega_{\rm GW}$ are negligible at the time of nucleosynthesis and we relate the amount of gravitational waves today to the reheating temperature and the time of equality between the kinetic scalar era and the radiation era.

We also pointed out that gravitational waves are damped by the anisotropic stress of radiation, which implies that the CMB anisotropy and polarization spectra are lowered roughly by 10% for high multipoles. It was also shown that the amplitude of the gravitational waves spectrum for inverse power law potentials is $\sim$30% higher than for SUGRA-like potentials at high frequency. Indeed this is probably not detectable by coming experiments but it could ultimately lead to a signature of supergravity.

ACKNOWLEDGMENTS

It is a pleasure to thank Pierre Binétruy, Nathalie Deruelle, Thibault Damour, David Langlois, Patrick Peter, and Filippo Vernizzi for fruitful discussions.

[1] A.G. Riess *et al.*, Astron. J. **116**, 1009 (1998).
[2] P.M. Garvanich *et al.*, Astrophys. J. **509**, 74 (1998).
[3] S. Perlmutter *et al.*, Nature (London) **391**, 51 (1998).
[4] A. Melchiorri *et al.*, astro-ph/9911445.
[5] Y. Mellier, Annu. Rev. Astron. Astrophys. **37**, 127 (1999).
[6] R. Juszkiewicz *et al.*, Science **287**, 109 (2000).
[7] N. Bahcall, J.P. Ostriker, S. Perlmutter, and P.J. Steinhardt, Science **284**, 1481 (1999).

[8] G. Efstathiou, Mon. Not. R. Astron. Soc. **310**, 842 (2000).
[9] S. Perlmutter, M.S. Turner, and M. White, Phys. Rev. Lett. **83**, 670 (1999).
[10] R.R. Caldwell, astro-ph/9908168.
[11] S. Weinberg, *Gravitation and Cosmology* (Wiley, New York, 1972).
[12] K. Coble, S. Dodelson, and J.A. Frieman, Phys. Rev. D **55**, 1851 (1997).
[13] R.R. Caldwell, R. Dave, and P.J. Steinhardt, Phys. Rev. Lett. **80**, 1582 (1998).
[14] P. Binétruy, Phys. Rev. D **60**, 063502 (1999).
[15] P. Brax and J. Martin, Phys. Lett. B **468**, 40 (1999).
[16] P. Brax and J. Martin, Phys. Rev. D **61**, 103502 (2000).
[17] C. Wetterich, Astron. Astrophys. **301**, 321 (1988).
[18] B. Ratra and P.J.E. Peebles, Phys. Rev. D **37**, 3406 (1988).
[19] P.J. Steinhardt, L. Wang, and I. Zlatev, Phys. Rev. D **59**, 123504 (1999).
[20] G. Huey, L. Wang, R. Dave, R.R. Caldwell, and P.J. Steinhardt, Phys. Rev. D **59**, 063005 (1999).
[21] I. Zlatev, L. Wang, and P.J. Steinhardt, Phys. Rev. Lett. **82**, 896 (1999).
[22] J.-P. Uzan, Phys. Rev. D **59**, 123510 (1999).
[23] N.D. Birrel and P.C.W. Davies, *Quantum Fields in Curved Space* (Cambridge University Press, Cambridge, England, 1982).
[24] L.H. Ford, Phys. Rev. D **35**, 2955 (1987).
[25] K. Maeda, Class. Quantum Grav. **3**, 233 (1986).
[26] F.S. Accetta, D.J. Zoller, and M.S. Turner, Phys. Rev. D **31**, 3046 (1985).
[27] F. Lucchin, S. Matarrese, and M.D. Pollock, Phys. Lett. **167B**, 163 (1986).
[28] L. Amendola, Phys. Rev. D **60**, 043501 (1999).
[29] S. Carroll, Phys. Rev. Lett. **81**, 3067 (1998).
[30] T. Chiba, Phys. Rev. D **60**, 083508 (1999).
[31] N. Bartolo and M. Pietroni, Phys. Rev. D **61**, 023518 (2000).
[32] O. Bertolami and P.J. Martins, Phys. Rev. D **61**, 064007 (2000).
[33] L.P. Grishchuk, Zh. Eksp. Teor. Fiz. **67**, 825 (1974) [Sov. Phys. JETP **40**, 409 (1974)].
[34] L.P. Grishchuk, Usp. Fiz. Nauk **156**, 297 (1988) [Sov. Phys. Usp. **31**, 940 (1988)].
[35] B. Allen, in *Relativistic Gravitation and Gravititional Radiation*, edited by J.-A. Marck and J.-P. Lasota (Cambridge University Press, Cambridge, England, 1997).
[36] A. Vilenkin and E.P.S. Shellard, *Cosmic Strings and Other Topological Defects* (Cambridge University Press, Cambridge, England, 1994).
[37] A. Abramovici *et al.*, Science **256**, 325 (1992).
[38] C. Bradaschia, Nucl. Instrum. Methods Phys. Res. A **289**, 518 (1990).
[39] Y.R. Jafry, J. Cornelisse, and R. Reinhard, ESA Bull. **18**, 219 (1994).
[40] V. Rubakov, M. Sazhin, and A. Veryaskin, Phys. Lett. **115B**, 189 (1982).
[41] A.A. Starobinsky, Pis'ma Astron. Zh. **9**, 579 (1983) [Sov. Astron. Lett. **9**, 302 (1983)].
[42] L.F. Abbott and M.B. Wise, Astrophys. J., Lett. Ed. **282**, L47 (1984).
[43] M. White, Phys. Rev. D **46**, 4198 (1992).
[44] M.S. Turner, M. White, and J.E. Lidsey, Phys. Rev. D **48**, 4613 (1993).
[45] W. Hu and M. White, New Astron. **2**, 323 (1997).
[46] M. Giovannini, Phys. Rev. D **60**, 123511 (1999).
[47] M. Giovannini, Class. Quantum Grav. **16**, 2905 (1999).
[48] P.J.E. Peebles and A. Vilenkin, Phys. Rev. D **59**, 063505 (1999).
[49] B. Spokoiny, Phys. Lett. B **315**, 40 (1993).
[50] M. Giovannini, Phys. Rev. D **59**, 121301 (1999).
[51] A. Melchiorri, M.V. Sazhin, V.V. Shulga, and N. Vittorio, Astrophys. J. **518**, 562 (1999).
[52] MAP, http://map.gsfc.nasa.gov/
[53] Planck, http://astro.estec.esa.nl/Planck/
[54] H. Kodama and M. Sasaki, Prog. Theor. Phys. Suppl. **78**, 1 (1984).
[55] J.-P. Uzan, Class. Quantum Grav. **15**, 1063 (1998).
[56] L.H. Ford and L. Parker, Phys. Rev. D **16**, 1601 (1977).
[57] C.W. Misner, K.S. Thorne, and J.A. Wheeler, *Gravitation* (Freeman, San Francisco, 1973).
[58] W. Hu and M. White, Phys. Rev. D **56**, 596 (1997).
[59] R.K. Sachs and A.M. Wolfe, Astrophys. J. **147**, 73 (1967).
[60] E. Newman and R. Penrose, J. Math. Phys. **7**, 863 (1966).
[61] J.N. Goldberg *et al.*, J. Math. Phys. **8**, 2155 (1967).
[62] K.S. Thorne, Rev. Mod. Phys. **52**, 299 (1980).
[63] P.J.E. Peebles, Astrophys. J. **153**, 1 (1968).
[64] S. Seager, D.D. Sasselov, and D. Scott, Astrophys. J. Lett. **523**, L1 (1999).
[65] C.-P. Ma and E. Bertschinger, Astrophys. J. **455**, 7 (1995).
[66] G.T. Gillies, Rep. Prog. Phys. **60**, 151 (1997).
[67] T. Damour and F. Dyson, Nucl. Phys. **B480**, 37 (1996).
[68] T. Damour and G. Esposito-Farese, Class. Quantum Grav. **9**, 2093 (1992).
[69] P.G. Ferreira and M. Joyce, Phys. Rev. D **58**, 023503 (1997).
[70] M. Tegmark and M. Zaldarriaga, Astrophys. J. (to be published), astro-ph/0002091.
[71] H. Ziaeepour, astro-ph/0002400.
[72] T. Chiba, T. Okabe, and M. Yamaguchi, Phys. Rev. D **62**, 023511 (2000).
[73] A. Dimitropoulos, Astron. Astrophys. Trans. **18**, 543 (1999).
[74] J. Silk, Astrophys. J. **151**, 459 (1968).
[75] W. Hu, Ph.D. thesis, University of California at Berkeley, 1995.
[76] L.P. Grishchuk, Phys. Rev. D **48**, 3513 (1993).
[77] M. Joyce, Phys. Rev. D **55**, 1875 (1997).
[78] L.P. Grishchuk, gr-qc/0002035.